Anisotropic structural modulation of epitaxial Au(111) thin films on striped Ag substrates

Puneet Mishra,* Takashi Uchihashi,† and Tomonobu Nakayama
International Center for Materials Nanoarchitectonics, National Institute for Materials Science, 1-1 Namiki, Tsukuba 305-0044, Japan
(Received 15 December 2009; revised manuscript received 19 February 2010; published 17 March 2010)

Au films grown on striped substrates [Ag/Si(111)-(4×1)-In] acting as an atomic-scale geometrical template were studied by scanning tunneling microscopy, low-energy electron diffraction and Auger electron spectroscopy. The "two-step growth" method, consisting of low-temperature deposition followed by a mild annealing to room temperature, was employed to form the Au films. The Au films grow in a layer-by-layer fashion on the atomically striped Ag substrates. Scanning tunneling microscope images reveal that the Au films are anisotropically modulated at the initial stage of the growth with stacking-fault induced steps on the Ag substrate. These steps, however, do not form uniformly throughout the surface, and their density decreases with increasing Au coverage due to higher stacking-fault energy of Au. These observations indicate the importance of low stacking-fault energy for the growth of atomic-scale periodic stripe structure.

DOI: 10.1103/PhysRevB.81.115430 PACS number(s): 68.55.−a, 68.37.Ef, 81.16.Dn

I. INTRODUCTION

Controlled fabrication of nanostructures, with tailored morphology as well as electronic properties, is an important aspect of current nanotechnology research. A promising route for the fabrication of functional nanostructures is the self-assembly of atoms and molecules on atomically well-defined surface templates.[1,2] This bottom-up approach aims to guide the assembly of adsorbates into surface structures with controlled shape, size and location through inherent processes such as adsorption, surface diffusion and nucleation. A variety of atomic-scale templates, e.g., reconstructed metal surfaces,[3] regular step arrays on vicinal surfaces[4,5] or semiconductor surfaces[6] have been utilized for self-assembly processes. However, such atomic-scale surface templates have not been fully utilized to control the atomic structure of the growing films.

The atomic structure of a growing film can be tailored by using a suitable template that introduces periodic defects in the crystal packing with high spatial density over large areas. Such long-range periodic defect arrays may modulate the periodic lattice potential of the film, thereby giving rise to novel electronic properties. Recently, the low-temperature (LT) grown Ag films on Si(111)-(4×1)-In [referred to as In-(4×1)] substrates were found to exhibit stripe structure with a transverse periodicity equal to that of the In chains of the substrate.[7] The stability of these stripes (up to 30 monolayer) has been attributed to a good lattice matching and small stacking-fault energy of Ag. Furthermore, angle-resolved photoelectron spectroscopy (ARPES) measurements on these striped Ag films have revealed the formation of quasi-one-dimensional (1D) electronic states.[8] They were found to have smaller binding energy compared to the isotropic Ag films with the same thickness, which has been attributed to the additional quantum confinement.[8]

Similar structural modulation and resultant quasi-1D confinement could be induced in other noble metals such as Au and Cu, owing to their relatively small stacking-fault energies.[9] In this context, the striped Ag substrate can be exploited as a template for the introduction of stripe structure into these metals by properly controlling the growth kinetics. The fact that the lattice parameters of Au are almost identical to those of Ag provides scope for the epitaxial growth of Au films on striped Ag substrates. Structural modulation of a Au film may significantly influence its electronic properties such as spin-split surface states due to the Rashba effect.[10]

In this paper, we report the morphological evolution of low-temperature grown Au films on Ag/In-(4×1) substrates. Our studies reveal that the Au films are anisotropically modulated at the early growth stage by the presence of stacking-fault induced steps parallel to the Ag stripes. The film growth occurs in a layer-by-layer fashion, and the film transforms into a Au(111) surface at higher coverage. For comparison, we have also grown Au films directly on In-(4×1) substrates. Growth behavior of Au films on this substrate is layer-by-layer but no well-defined Au(111) surfaces are formed.

II. EXPERIMENTAL METHODS

Our experiments were performed in an ultrahigh vacuum chamber equipped with a low-energy electron diffraction (LEED), an Auger electron spectroscopy (AES) apparatus and a scanning tunneling microscope (STM). First, a Si(111)-7×7 clean surface was prepared by high temperature flashing up to 1300 °C. A small amount of indium [~1.8 monolayer (ML)] was deposited on the surface followed by sample annealing in the temperature range of 340–360 °C for 5 min to obtain a well-developed In-(4×1) surface.[11] For the growth of Ag and Au films, we employed the "two-step growth" method consisting of (i) a LT vacuum deposition at 110 K, followed by (ii) a natural annealing to room temperature (RT).[12–14] For LT deposition, the diffusion is limited and there is an accumulation of disorder and strain. Such imperfections drive the atomic redistribution and recrystallization of the as-deposited disordered film during annealing. This method enables the growth of atomically flat metal thin films on semiconductor substrates. Additionally, deposition at LT effectively suppresses the intermixing between the growing layer and the substrate. For the growth of Au films, a shadow mask was placed in front of the sample to fabricate a wedge structure with a continu-

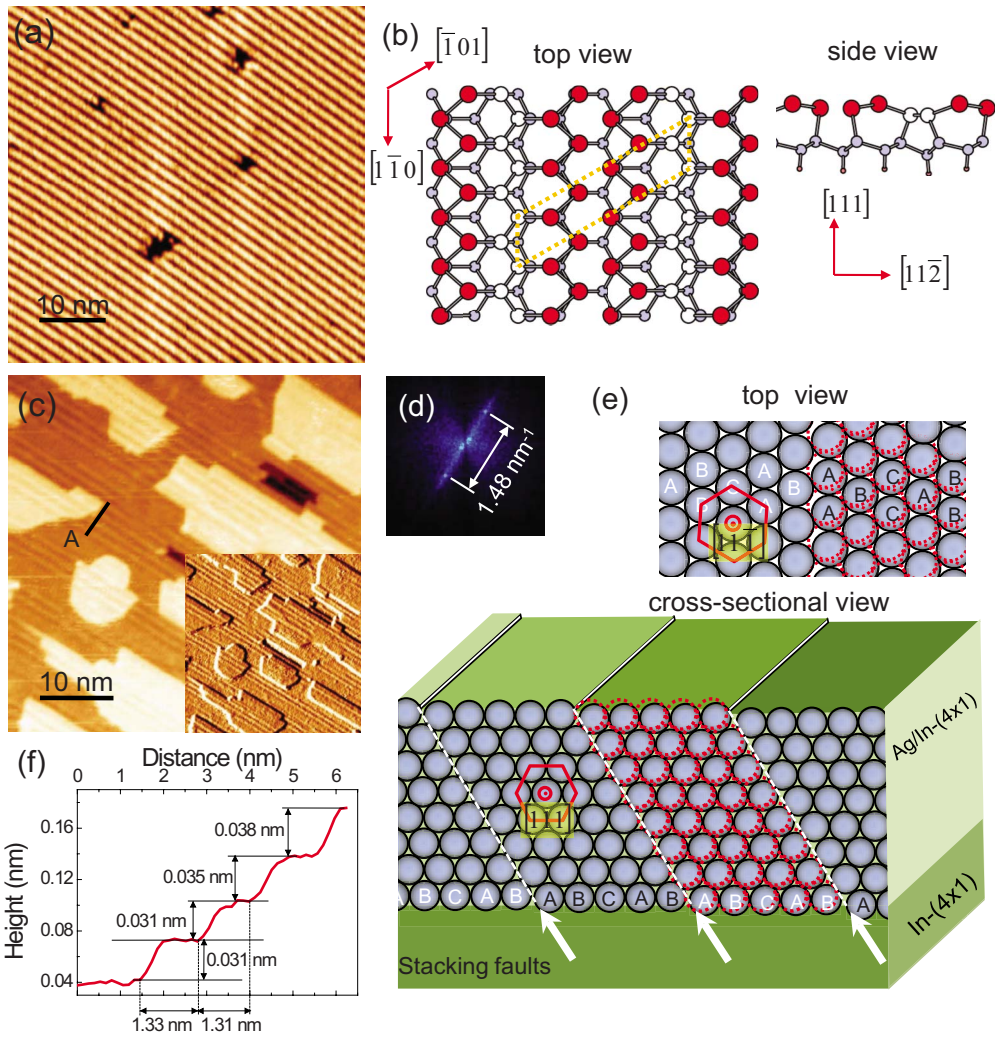

FIG. 1. (Color online) (a) STM image of a In-(4×1) surface (V_{tip}=+2.0 V, I_t=0.1 nA). (b) The atomic structure model of the In-(4×1) reconstruction (left panel: top view, right panel: side view). The red (dark gray in print) circles represent In atoms, while the white and the light gray circles represent Si atoms. The In-(4×1) surface unit cell containing 4 In atoms is sketched by the dotted line. (c) STM image of a Ag film of thickness 6 ML. Inset shows the derivative STM image of the same region (V_{tip}=−1.5 V, I_t=0.1 nA). (d) Power spectrum of the Fourier transformation of the STM image shown in Fig. 1(c). (e) A schematic illustration of the atomic structure model of Ag stripes (upper panel: top view, lower panel: cross-sectional view) (Ref. 7). The dotted circles show the unfaulted position of the Ag atoms. The dashed lines along the arrows indicate the stacking-fault lines. (f) A tilt-corrected height profile along line A in Fig. 1(c).

ous change in film thickness.[7,15] This technique allows us to directly determine the local film thickness and to correlate it with the morphology through the STM observations. The STM images of these Au films exhibit negligible bias voltage dependence, thus representing the morphology of the layer. All STM measurements were performed at RT.

III. RESULTS AND DISCUSSION

A. Growth of striped Ag films on In-(4×1) substrate

An In-(4×1) surface was adopted as a template for the growth of Ag films due to its strong 1D anisotropy.[16–19] Figure 1(a) shows an STM image (V_{tip}=2.0 V, I_t=0.1 nA) of the In-(4×1) surface exhibiting linear In chains. These In chains run parallel to the [1$\bar{1}$0] axis of the bulk Si with a periodicity of 1.33 nm. The atomic structure model of the In-(4×1) reconstructed surface is shown in Fig. 1(b). It consists of two zigzag chains of In atoms separated by a Si chain on the surface of an almost undistorted Si substrate.[19] Due to the covalent bonding between In and Si atoms at the In-Si interface, the linear chain structure of the surface may not be disrupted even after being buried with a metal film.

The STM image of a 6 ML Ag film on In-(4×1) surface is shown in Fig. 1(c). The image reveals two distinct features: (i) the surface of the Ag film consists of equally spaced stripes parallel to the In chain direction, and (ii) Ag islands are elongated along the stripe direction.[7] In order to enhance the contrast, we have processed the STM image by taking the deviation of the tip height z, with respect to the fast scan direction x, i.e., dz/dx. The resulting derivative STM image of the same region is shown in the inset. The power spectrum of the STM image [Fig. 1(d)] shows two bright spots separated by 1.48±0.09 nm^{-1}, which reveals the periodicity of

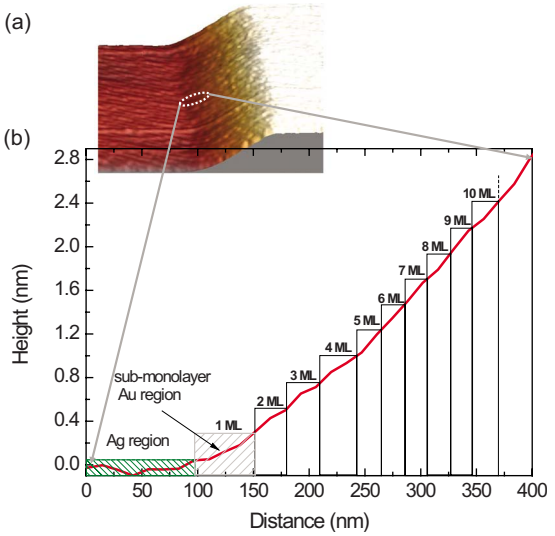

FIG. 2. (Color online) (a) A 3D STM image of a wedge structure fabricated by placing a shadow mask during Au deposition. (b) The average height variation of the Au film near the Ag-Au boundary. The continuous increase in average thickness is labeled from Ag region up to 10 ML thick Au region.

the stripe structure to be 1.35 ± 0.08 nm similar to that of the In chains. These observations indicate that the growing Ag layers follow the corrugations of the indium chains.

A schematic illustration of the atomic structure model of the film is shown in Fig. 1(e).[7] The close-packed Ag atoms of one of the $\langle 111 \rangle$ planes are stacked as $..ABCAB|ABCAB..$, with a stacking fault at the position indicated by the symbol "|." The stripe structures consist of surface nanoplanes of Ag(111), which are separated from each other by steps of 0.078 nm in height. Here, these steps are referred to as fractional steps because the height corresponds to 1/3 of the Ag(111) monoatomic step height. On a stepped surface, the terraces generally appear with some slope in the STM images due to the inclination of the tip with respect to the sample. The slope becomes larger if the scan size is significantly more than the terrace width. In order to elucidate the actual stepped nature of the surface, it is necessary to perform plane fitting on atomically flat terraces. We refer this procedure as "tilt-correction" of the height profile. Figure 1(f) depicts the tilt-corrected height profile measured along line A in Fig. 1(c), showing fractional steps of 0.03–0.04 nm in height. These fractional steps generally appear to be reduced in height because of the small periodicity of the stripes and finite size of the STM tip.[20]

B. Growth of Au film on striped Ag substrates

We adopted a 6 ML striped Ag film as a template for the growth of Au films. Repeated experiments including striped Ag films with a thickness of 2–3 ML basically gave the same results. A three-dimensional (3D) STM image of a wedge structure, fabricated to facilitate the observation of continuous change in the film thickness, is shown in Fig. 2(a). Au film thickness at the maximum height was estimated to be 12.5 nm. Figure 2(b) shows the variation of the average height of the Au film near the boundary. The nominal film coverage indicated in Fig. 2(b) was determined by assuming that the interlayer distance of the film was equal to its bulk value along [111] direction (1 ML=0.236 nm). We have performed a careful creep correction before assigning the coverage value to an image at any specific location. The error in the coverage determination is estimated to be less than 1 ML.

The evolution of the surface morphology versus Au coverage is depicted in the STM images presented in Figs. 3(a) and 3(c). In order to elucidate the small structural features of the surface, the corresponding derivative STM images are presented in Figs. 3(b) and 3(d), respectively. The local film thickness in units of ML is indicated on the left side of each STM image. The film growth occurs in a layer-by-layer fashion, although the growth is not ideal and the formation of a new layer starts before the preceding layer is complete. More importantly, the morphology of the Au film shows the presence of straight steps running parallel to the Ag stripes. Some of these steps on the top surface are periodically aligned with the same periodicity as those on the Ag region. The height profiles [Fig. 3(e)] of the Ag-stripes (line L1) and those of the striped Au regions at 2 ML (line L2) and 3 ML (line L3) show a good matching in periodicity. Figure 3(f) shows a tilt-corrected height profile measured on a terrace with separated steps (line L4). The measured step height is close to the fractional step height (=0.078 nm) calculated for the striped Ag surface. These observations demonstrate that such straight steps are indeed stacking-fault induced fractional steps [Fig. 3(g)]. Note that the Au films exhibit anisotropic islands with straight edges which are aligned along the direction of Ag stripes. Such island shape anisotropy was also observed in the case of the Ag films grown on In-(4×1) surfaces, which was attributed to step-guided surface atom diffusion.[7] To summarize, the Au film is anisotropically modulated in the early growth stage by the presence of the striped Ag substrate.

However, the fractional steps on the Au surface do not distribute uniformly as those on the Ag substrate. Flat regions are visible even at 1 ML and they constitute a significant fraction of the total surface area. Furthermore, the density of fractional steps on the Au surface decreases with increasing coverage. Extensive STM observations confirmed that they completely disappear beyond 18 ML. Moreover, the stripes at higher Au coverages become wider than the Ag stripes. Figure 3(h) shows the stripe width distributions for the dashed rectangular regions designated as (i), (ii) and (iii). Here, we define a stripe as a terrace confined between adjacent fractional steps. The surface exhibits a uniform stripe width of 1.3 nm up to 2 ML [cf., histogram (i)], which is similar to the Ag stripe width. However, as the coverage increases [cf., histograms (ii) and (iii)], the fraction of the wider stripes becomes comparable to that of the Ag-like stripes. Although our analysis is performed on a limited region of the film, it represents the qualitative behavior of the Au surface evolution with coverage.

The decrease in the density of fractional steps and the appearance of wider stripes indicate that the periodic insertion of stacking faults in the Au film is energetically unfavorable. In literature, the values for intrinsic stacking-fault

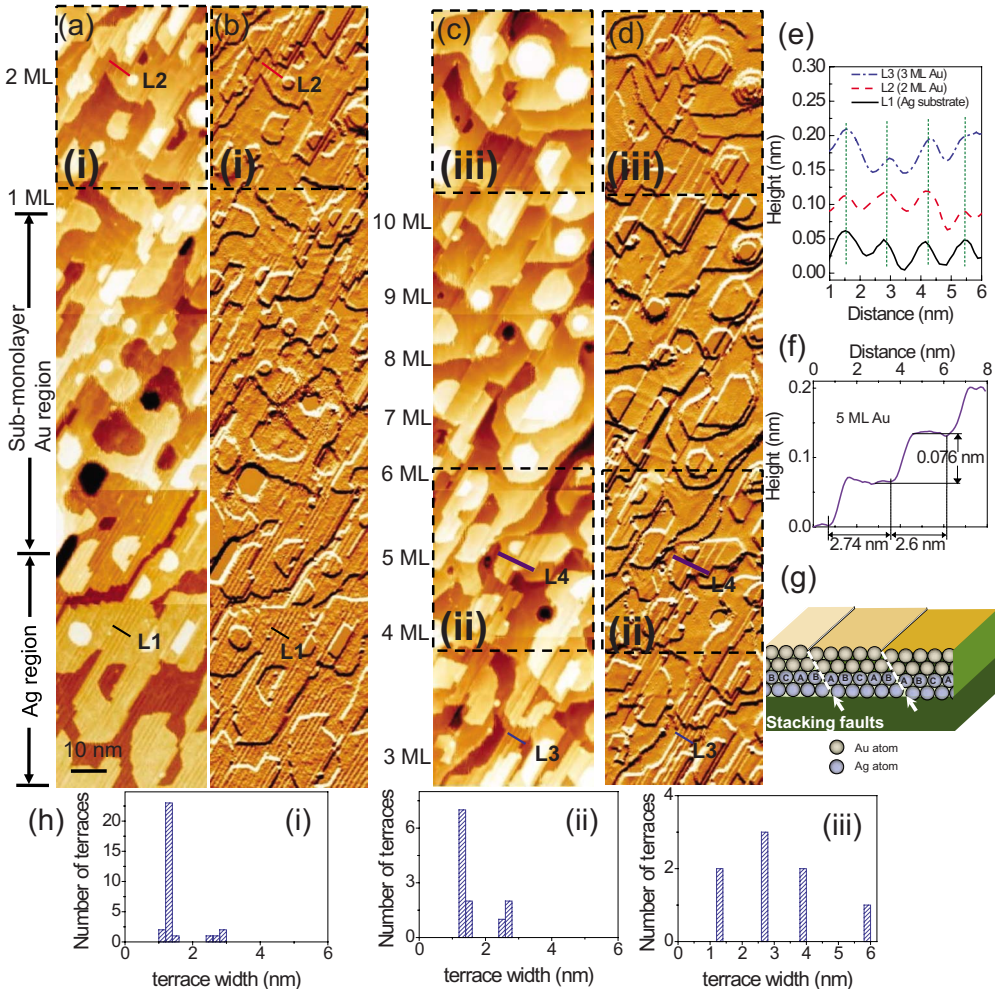

FIG. 3. (Color online) STM images (a, c) and derivative STM images (b, d) of a wedge shaped Au film. The local thickness of the film in units of ML is indicated on the left side of the topography images (V_{tip}=−1.5 V, I_t=0.1 nA). (e) Height profiles measured along lines L1 (Ag stripes), L2 (2 ML Au film) in Fig. 3(a) and L3 (3 ML Au film) in Fig. 3(c). (f) Tilt-corrected height profile along L4 (5 ML Au film) in Fig. 3(c) showing fractional atomic steps. (g) Schematic illustration of the atomic structure model (cross-sectional view) of the Au film on Ag stripes. The dashed lines along the arrows indicate the stacking-fault lines. (h) Stripe width histograms for the regions (i), (ii), and (iii) marked with dashed rectangles in Figs. 3(a) and 3(c).

energy (γ_{sf}) per unit area for Au have been reported to be 29 to 59 mJ/m^2.[21,22] This is almost a factor of two larger than that for Ag.[23] Higher stacking-fault energy for Au can be responsible for the observed trends in the density of fractional steps and their separation.

In the following, we have adopted the thermodynamic model given by Liu *et al.*[24] to predict the thickness dependent stripe structure stability. The condition for the existence of stable stripe structures in a Au film is that the energy cost due to the presence of stacking faults and the strain in the film is sufficiently lower than the energy gain at the interface. Neglecting the entropy gain associated with the structural transition from a striped structure to flat surface,[25] the equilibrium condition, i.e., $U_e+U_{sf}=U_{in}$ leads to a critical thickness up to which the stripe structure exists. Here, U_e is the elastic energy, U_{sf} is the stacking-fault energy in the film and U_{in} is the incoherent film-substrate interface energy. Using the classical elastic theory and a thermodynamic model for the film-substrate interface energy, the critical film thickness n_c (in ML units) at the equilibrium condition is given by[24]

$$n_c = \frac{4\bar{h}\bar{S}_{vib}\bar{H}_m}{3\bar{V}_m R} \times \left\{ \frac{d\epsilon_{in}^2 E_f}{[6(1-\nu_f)]} + \frac{\gamma_{sf}}{n_{sr}} \right\}^{-1}, \qquad (1)$$

where h is the nearest-neighbor atomic distance, S_{vib} is the vibrational component of the bulk melting entropy, H_m is the melting enthalpy of the crystal, V_m is the molar volume and R is the ideal gas constant. Furthermore, d is the distance between the adjacent (111) planes, ϵ_{in} is the strain and E_f and ν_f are the elastic modulus and the Poisson's ratio of the film, respectively. The symbol "–" over a physical quantity denotes the mean value of the film and the substrate. Substituting the values of thermodynamic parameters from literature[24,26] and noting that the number of close-packed (111) planes in every stripe n_{sr}=5 for the Ag films,[7] the critical thickness for Ag stripe structure on In-(4×1) substrate is determined to be 20 ML. Using the above formalism, the

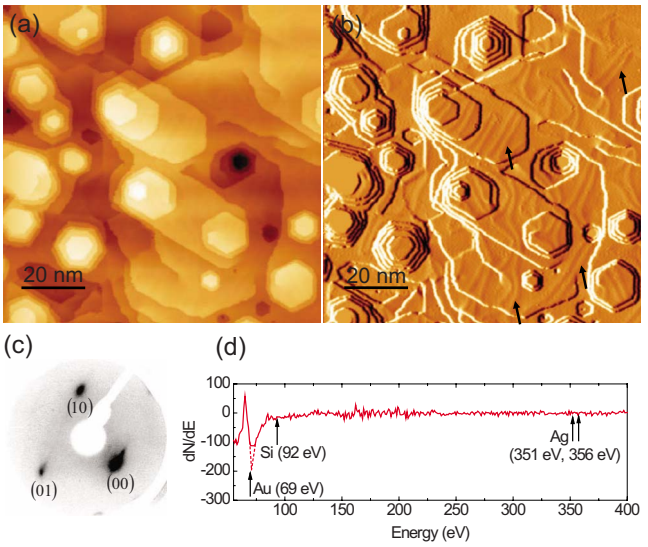

FIG. 4. (Color online) STM image (a) and derivative STM image (b) of a 50 ML thick Au film. (c) LEED pattern and (d) AES spectrum of a 12 ML Au film on Ag/In-(4×1) substrate. The dotted line which extends the saturated Au signal is drawn to guide the eye.

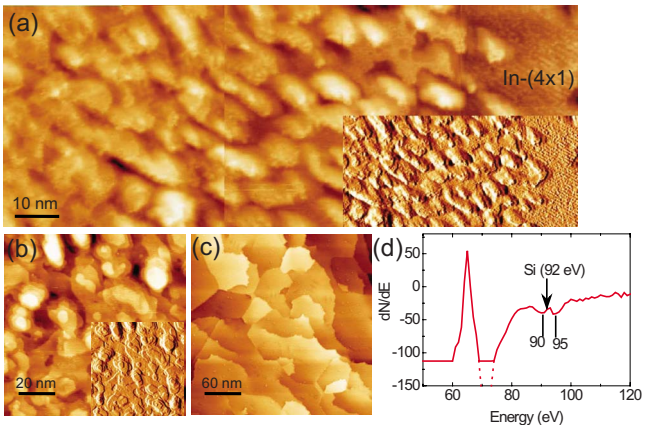

FIG. 5. (Color online) (a) STM image of a wedge shaped Au film grown on In-(4×1) substrate. Inset shows the corresponding derivative STM image. (b) STM image of a 50 ML thick Au film. The derivative STM image is shown in the inset. (c) STM image of a 50 ML thick Au film after annealing. (d) AES spectrum of a Au film on In-(4×1) substrate. The dotted line which extends the saturated Au signal is drawn to guide the eye.

critical thickness of Au films on 6 ML striped Ag/In-(4×1) substrates is estimated to be 11 ML. Here, we assume that among the Ag-In and Au-Ag interfaces, the one with a lower interface energy will determine the thermodynamic equilibrium condition.

These results are reasonably consistent with the observed critical thickness of 30 ML in Ag films[7] and 18 ML in Au films on Ag/In-(4×1) substrates. In fact, the values calculated using Eq. (1) can be considered as the lower limit for the critical thickness in a film since it takes into account only the thermodynamic equilibrium criterion. However, growth of thin films is intrinsically a nonequilibrium phenomenon governed by a competition between kinetics and thermodynamics. The state which is obtained is not necessarily the most stable but is kinetically determined. The kinetic parameters can cause substantial hysteresis in the structural transition leading to a larger value of the experimentally observed critical thickness.

An experimental observation of the structure evolution from a metastable state (e.g., stripes) at low coverage to fully relaxed (stable) state at higher coverage provides physical insight into the growth mechanism of a specific adlayer-substrate system. At higher Au coverage, anisotropic surface modulations disappear and the surface of the Au film finally transforms into that of Au(111). For a film with a thickness of more than 10 ML, the surface exhibits hexagonal islands which are representative of a Au(111) surface.[27] A typical STM image of the film surface at 50 ML thickness is shown in Fig. 4(a). In addition to the hexagonal islands, the moderately wide terraces exhibit pairs of lines, which are attributed to the herringbone structure [indicated by arrows in the derivative STM image in Fig. 4(b)]. Such a double line arrangement originates from the presence of intrinsic tensile stress in the outermost layer of a pure, close-packed Au(111) surface.[28] LEED measurements [Fig. 4(c)] provide further evidence for the presence of Au(111) surface. The diffraction spots are elongated, which is due to the residual anisotropic modulation of the Au films.

AES investigations of the Au films yielded no evidence for surface segregation of substrate species. Figure 4(d) shows an AES spectrum obtained on a 12 ML Au film with a prominent Au peak at 69 eV. At a thickness of 12 ML Au overlayer, the Ag Auger signal is estimated to be suppressed compared to that of a very thick Ag layer by a factor of about 60.[29–31] Consequently, no peaks corresponding to Ag (351 and 356 eV) or Si (92 eV) were detected, within the accuracy of the measurements. Ideally, Au(111) films are expected to grow epitaxially on Ag(111) surface in a layer-by-layer fashion, owing to their good lattice matching, comparable surface energies[32] and low bulk diffusion coefficients.[33,34] Although sharp Au-Ag interface with high structural quality has been widely reported,[35–39] there are several reports, which contradict the above ideal picture and suggest the occurrence of Au-Ag intermixing.[40–43] Our AES spectra demonstrate that the top surface is comprised of pure Au and the segregation of Ag or Si to the surface does not occur. This may be a direct consequence of the LT deposition employed in our studies.[13,14]

C. Growth of Au films on In-(4×1) substrates

The Au films grown on In-(4×1) substrates show strikingly different topographical features from those observed on the striped Ag substrates. Figure 5(a) shows an STM image and its lateral derivative (shown in the inset) of a wedge shaped Au film. The In-(4×1) surface is visible on the rightmost side of the image. While the film growth occurs in a layer-by-layer fashion, fractional steps, and anisotropic islands are lacking on the surface of these Au films. A comparison of the growth of Au and Ag films on In-(4×1) substrate further reveals significant differences. In contrast to Ag [cf., Fig. 1(c)], even the first few Au layers do not show any

signature of growth anisotropy along the In-atomic chains. This may be attributed to the lower surface diffusivity of Au as compared to that of Ag.[44] These observations show the importance of the striped Ag surface as a template for the growth of anisotropically modulated Au films.

At higher coverage, the Au films do not exhibit a pure Au(111) surface. An STM image of a 50 ML thick Au film is shown in Fig. 5(b). No evidence of hexagonal islands and herringbone pattern was found in the STM images. Additionally, no clear diffraction spots were observed in LEED measurements. Annealing of these films in the temperature range of $150\,^{\circ} \leq T \leq 250\,^{\circ}$C results in a very flat surface with large terrace widths [Fig. 5(c)]. However, neither clear LEED spots nor herringbone pattern were observed. Figure 5(d) shows an AES spectrum obtained on this surface exhibiting Si peaks at 90 and 95 eV. The appearance of the two peaks, instead of the characteristic Auger peak of Si at 92 eV, indicates the formation of gold silicide.[45] These results demonstrate the occurrence of appreciable Si diffusion into Au films. Referring to the atomic structure model shown in Fig. 1(b) (side view), the In-(4×1) surface consists of both In and Si atoms. The Si atoms which are exposed on the surface may readily diffuse into the Au film leading to the formation of a disordered surface layer containing a mixture of Au and Si. This may be a reason for the absence of the hexagonal islands, herringbone pattern and clear LEED spot on Au films grown on In-(4×1) substrates.

IV. CONCLUSIONS

We have shown that the structure of the Au films grown on Ag/In-(4×1) surfaces is anisotropically modulated at the early growth stage due to quasi-1D nature of the substrate. The surface exhibits elongated islands up to 10 ML and fractional steps due to stacking faults up to 18 ML. However, the fractional steps do not form uniformly throughout the surface, and their density decreases with increasing Au coverage. This behavior can be attributed to the higher stacking-fault energy of Au compared to that of Ag. The Au film grows in a layer-by-layer fashion and exhibits a pure Au(111) surface at higher coverages. The absence of anisotropic modulation in Au films grown directly on In-(4×1) substrates shows the importance of striped Ag surface as a template.

ACKNOWLEDGMENTS

This work was supported by World Premiere International Research Center Initiative on Materials Nanoarchitectonics, MEXT, Japan. We acknowledge the financial support from the Iketani Science and Technological Foundation and JSPS Grant-in-Aid for Scientific Research (Grant No. 21510110) from the Japanese Society for the Promotion of Science. We also thank T. Okuda for fruitful discussions.

*mishra.puneet@nims.go.jp
†uchihashi.takashi@nims.go.jp

[1] J. V. Barth, G. Costantini, and K. Kern, Nature (London) **437**, 671 (2005).
[2] C. Tegenkamp, J. Phys.: Condens. Matter **21**, 013002 (2009).
[3] M. Böhringer, K. Morgenstern, W.-D. Schneider, R. Berndt, F. Mauri, A. De Vita, and R. Car, Phys. Rev. Lett. **83**, 324 (1999).
[4] P. Gambardella, A. Dallmeyer, K. Maiti, M. C. Malagoli, W. Eberhardt, K. Kern, and C. Carbone, Nature (London) **416**, 301 (2002).
[5] P.-G. Kang, H. Jeong, and H. W. Yeom, Phys. Rev. B **79**, 113403 (2009).
[6] J.-L. Li, J.-F. Jia, X.-J. Liang, X. Liu, J.-Z. Wang, Q.-K. Xue, Z.-Q. Li, J. S. Tse, Z. Zhang, and S. B. Zhang, Phys. Rev. Lett. **88**, 066101 (2002).
[7] T. Uchihashi, C. Ohbuchi, S. Tsukamoto, and T. Nakayama, Phys. Rev. Lett. **96**, 136104 (2006).
[8] N. Nagamura, I. Matsuda, N. Miyata, T. Hirahara, S. Hasegawa, and T. Uchihashi, Phys. Rev. Lett. **96**, 256801 (2006).
[9] M. J. Mehl, D. A. Papaconstantopoulos, N. Kioussis, and M. Herbranson, Phys. Rev. B **61**, 4894 (2000).
[10] S. LaShell, B. A. McDougall, and E. Jensen, Phys. Rev. Lett. **77**, 3419 (1996).
[11] T. Uchihashi and U. Ramsperger, Appl. Phys. Lett. **80**, 4169 (2002).
[12] L. Huang, S. J. Chey, and J. H. Weaver, Surf. Sci. Lett. **416**, L1101 (1998).
[13] M. Horn–von Hoegen, T. Schmidt, G. Meyer, D. Winau, and K. H. Rieder, Phys. Rev. B **52**, 10764 (1995).
[14] G. Meyer and K. H. Rieder, Surf. Sci. **331-333**, 600 (1995).
[15] T. Uchihashi, T. Nakayama, and M. Aono, Jpn. J. Appl. Phys. **46**, 5975 (2007).
[16] J. Kraft, M. G. Ramsey, and F. P. Netzer, Phys. Rev. B **55**, 5384 (1997).
[17] G. Lee, S.-Y. Yu, H. Kim, J.-Y. Koo, H.-I. Lee, and D. W. Moon, Phys. Rev. B **67**, 035327 (2003).
[18] J. J. Lander and J. Morrison, J. Appl. Phys. **36**, 1706 (1965).
[19] O. Bunk, G. Falkenberg, J. H. Zeysing, L. Lottermoser, R. L. Johnson, M. Nielsen, F. Berg-Rasmussen, J. Baker, and R. Feidenhans'l, Phys. Rev. B **59**, 12228 (1999).
[20] S. Dongmo, P. Vautrot, N. Bonnet, and M. Troyon, Appl. Phys. A: Mater. Sci. Process. **66**, S819 (1998).
[21] N. Bernstein and E. B. Tadmor, Phys. Rev. B **69**, 094116 (2004).
[22] N. M. Rosengaard and H. L. Skriver, Phys. Rev. B **47**, 12865 (1993).
[23] J. Cai and J.-S. Wang, Modell. Simul. Mater. Sci. Eng. **10**, 469 (2002).
[24] D. Liu, M. Zhao, and Q. Jiang, Appl. Surf. Sci. **253**, 3586 (2007).
[25] I. Daruka and A.-L. Barabási, Appl. Phys. Lett. **72**, 2102 (1998).
[26] http://www.webelements.com.
[27] L. Zhang, F. Cosandey, R. Persaud, and T. E. Madey, Surf. Sci. **439**, 73 (1999).
[28] J. V. Barth, H. Brune, G. Ertl, and R. J. Behm, Phys. Rev. B **42**, 9307 (1990).
[29] M. P. Seah and W. A. Dench, Surf. Interface Anal. **1**, 2 (1979).

[30] S. Tanuma, C. J. Powell, and D. R. Penn, Surf. Interface Anal. **17**, 911 (1991).
[31] C. J. Powell and A. Jablonski, J. Phys. Chem. Ref. Data **28**, 19 (1999).
[32] J. H. van der Merwe and E. Bauer, Phys. Rev. B **39**, 3632 (1989).
[33] F. Soria and J. L. Sacedón, Thin Solid Films **60**, 113 (1979).
[34] B. Gruzza, J. M. Guglielmacci, and E. Gillet, Thin Solid Films **52**, 103 (1978).
[35] T. Miller, A. Samsavar, G. E. Franklin, and T.-C. Chiang, Phys. Rev. Lett. **61**, 1404 (1988).
[36] T. Miller, M. A. Mueller, and T.-C. Chiang, Phys. Rev. B **40**, 1301 (1989).
[37] R. J. Culbertson, L. C. Feldman, P. J. Silverman, and H. Boehm, Phys. Rev. Lett. **47**, 657 (1981).
[38] T. C. Hsieh, T. Miller, and T.-C. Chiang, Phys. Rev. Lett. **55**, 2483 (1985).
[39] F. J. Palomares, M. Serrano, A. Ruiz, F. Soria, K. Horn, and M. Alonso, Surf. Sci. **513**, 283 (2002).
[40] U. Lipphardt, H. Engelhard, J. Westhof, A. Goldmann, and S. Witzel, Surf. Sci. **294**, 84 (1993).
[41] B. Eisenhut, J. Stober, G. Rangelov, and Th. Fauster, Phys. Rev. B **49**, 14676 (1994).
[42] S. Chiang, S. Rousset, D. E. Fowler, and D. D. Chambliss, J. Vac. Sci. Technol. B **12**, 1747 (1994).
[43] E. S. Hirschorn, T. Miller, M. Sieger, and T.-C. Chiang, Surf. Sci. Lett. **295**, L1045 (1993).
[44] S. M. Foiles, M. I. Baskes, and M. S. Daw, Phys. Rev. B **33**, 7983 (1986).
[45] K. Oura and T. Hanawa, Surf. Sci. **82**, 202 (1979).